

Supporting Information

Oxidative *trans* to *cis* Isomerization of Olefins in Polyketide Biosynthesis

*Tsuyoshi Yamamoto, Yuta Tsunematsu, Kodai Hara, Tomohiro Suzuki, Shinji Kishimoto, Hirokazu Kawagishi, Hiroshi Noguchi, Hiroshi Hashimoto, Yi Tang, Kinya Hotta, and Kenji Watanabe**

anie_201600940_sm_miscellaneous_information.pdf

Table of Contents

| | |
|---|--------|
| 1. Supporting Methods | S2–S7 |
| 1.1 Reagents, strains and general techniques for DNA manipulation. | S2 |
| 1.2 Construction of pKW20271 for expression of <i>psoE</i> | S2–S3 |
| 1.3 Production and purification of PsoE. | S3–S4 |
| 1.4 Production and purification of SeMet-substituted PsoE. | S4 |
| 1.5 <i>In vitro</i> analysis of the activity of PsoE and PsoF against 5 | S4–S5 |
| 1.6 Additional <i>in vitro</i> analyses of the activities of PsoE and PsoF. | S5–S6 |
| 1.7 Protein crystallization and data collection. | S6 |
| 1.8 Structure refinement and model completion. | S6 |
| Table S1. Oligonucleotide primer sequences. | S7 |
| | |
| 2. Supporting Results | S8–S15 |
| 2.1 <i>E. coli</i> production of PsoE. | S8 |
| 2.2 Additional <i>in vitro</i> analyses of the activities of PsoE and PsoF. | S9–S10 |
| 2.3 Glutathione-binding domain of amino acid sequence alignment. | S11 |
| 2.4 Comparison of the ligand-binding mode in different GSTs..... | S12 |
| 2.5 Effect of cobalt ion on packing of the ligand by PsoE. | S13 |
| Table S2. Data and structural refinement statistics on the PsoE–GSH– 5 complex crystallized with cobalt ion. | S14 |
| Table S3. Data and structural refinement statistics on the PsoE–GSH– 5 complex crystallized without cobalt ion. | S15 |
| | |
| 3. Supporting References | S16 |

1. Supporting Methods

1.1 Reagents, strains and general techniques for DNA manipulation.

All chemicals were purchased from Sigma-Aldrich and Wako Pure Chemical Industries, Ltd. unless otherwise specified. Purchased chemicals were of reagent grade and used without further purification. *Aspergillus fumigatus* A1159, a producer of pseurotins, was obtained from the Fungal Genetics Stock Center, USA. *E. coli* XL1-Blue (Agilent Technologies) and *E. coli* TOP10 (Thermo Fisher Scientific) were used for plasmid propagation by standard procedures. Overproduction of recombinant proteins was carried out in *E. coli* BL21 (DE3) (Thermo Fisher Scientific). DNA restriction enzymes were used as recommended by the manufacturer (Fermentas). PCR was carried out using PrimeSTAR GXL DNA polymerase (TAKARA Bio Inc.) as recommended by the manufacturers. Sequences of PCR products were confirmed through DNA sequencing (Macrogen Japan Corporation). PCR was performed with the *A. fumigatus* cDNA as a template to amplify the target gene using primer sets listed in **Table S1**. Details of the plasmid construction are given below, and the plasmid map is shown in **Figure S1**.

1.2 Construction of pKW20271 for expression of *psoE*.

The open reading frame (ORF) of the pseurotin biosynthetic genes was predicted based on the *A. fumigatus* genome sequence information available from the National Center for Biotechnology Information (NCBI) database, and their predicted function was determined by comparison to known proteins using the BLAST peptide sequence database search program¹, Conserved Domain Database search² and the FFAS03 protein sequence profile-profile alignment and fold recognition program³. The correct 5' and 3' ends of the gene were determined successfully and the corresponding cDNA was prepared using essentially the same 5' and 3' RACE method described in our previous report⁴ for constructing vectors for expression of the gene in *E. coli*. The *psoE* gene was amplified using the cDNA as a template by PCR with two primers pKW20271-F1/pKW20271-R1 (**Table S1**) and ligated with the pET21c(+) expression vector (EMD Millipore Corporation) that was digested with *Nde* I (10 units) and *Xho* I (10 units) to generate pKW20271 (**Figure S1A**) using GeneArt Seamless Cloning and Assembly kit (Thermo Fisher Scientific). The identity of the resulting vector pKW20271 was confirmed by DNA sequencing (Macrogen Japan Corporation). This plasmid

was used to express *psoE* for preparing purified samples of recombinant PsoE to be used in *in vitro* assays and crystallization.

1.3 Production and purification of PsoE.

Overexpression and subsequent protein purification of PsoE was performed as follows: BL21(DE3) harboring plasmid pKW20271 was grown overnight in 20 ml of LB medium with 100 µg/ml ampicillin at 37 °C. Five liters of fresh LB medium with 100 µg/ml ampicillin was inoculated with 20 ml of the overnight culture and incubated at 37 °C until the optical density at 600 nm (OD₆₀₀) reached 0.6. Then expression of the gene was induced with 100 µM isopropylthio-β-D-galactoside (IPTG) at 15 °C. Incubation was continued for another 24 h, after which cells were harvested by centrifugation at 10,000 × g for 10 min. All subsequent procedures were performed at 4 °C or on ice. Harvested cells were resuspended in disruption buffer (0.1 M Tris-HCl at pH 7.4, 0.1 M NaCl and 20 mM imidazole). Cells were disrupted by French Press, and the lysate was clarified by centrifugation at 10,000 × g for 10 min. The supernatant and precipitate were recovered as the soluble and insoluble fraction, respectively. The soluble fraction containing protein was applied onto a Ni Sepharose 6 Fast Flow (GE Healthcare) column. After washing the column with 10 mM imidazole and 0.1 M NaCl in 0.1 M Tris-HCl pH 7.4, the target protein was eluted with 0.1 to 1.0 M imidazole and 0.1 M NaCl in 0.1 M Tris-HCl pH 7.4. Further purification was carried out on an anion-exchange column (HiTrap Q, 5 ml × 2, GE Healthcare). A gradient of 0–1 M NaCl in 50 mM Tris-HCl (pH 8.5) was applied at a flow rate of 2 ml/min over 95 min. Fractions of 2 ml were collected, and fractions with the desired protein, which typically eluted at 0.3 M NaCl, were pooled and further concentrated with Amicon Ultra centrifugal concentrator (EMD Millipore Corporation). Then the protein was further purified by Superdex 75 gel filtration (16 × 600 mm, GE Healthcare) in a buffer containing 10 mM Tris-HCl, pH 7.4 and 0.1 M NaCl at a flow rate 1 ml/min. The purified proteins in 10 mM Tris-HCl (pH 7.4) and 0.1 M NaCl were pooled and concentrated to a concentration of 25 mg/ml with Amicon Ultra centrifugal concentrator. Protein concentration was estimated using the Bio-Rad protein assay kit with bovine serum albumin as a standard. This sample was analyzed by sodium dodecyl sulfate (SDS)–polyacrylamide gel electrophoresis (PAGE) using Tris-HCl 10% of polyacrylamide gel stained with Coomassie Brilliant Blue R-250 stain solution (CBB; nacalai tesque) (**Figure S1B**). Purified PsoF was prepared following essentially the same procedure described in our

previous report⁵. Purified protein sample was clearly yellow in color, indicating that PsoF contains a flavin cofactor.

1.4 Production and purification of SeMet-substituted PsoE.

The BL21(DE3) harboring plasmid pKW20271 was cultured overnight at 37 °C in 25 ml of M9 minimal medium containing 100 µg/ml ampicillin. This overnight culture was centrifuged at a 5,000 × *g* for 1 min to collect the cells. The cells were washed with sterilized water and M9 minimal medium, and resuspended in M9 minimal medium to inoculate a total of 4 l of M9 minimal medium in a fermentation vessel. After 9 h of incubation at 37 °C with agitation at 800 rpm, an OD₆₀₀ of 0.3 was achieved. After addition of 100 mg/l of L-lysine, 100 mg/l of L-phenylalanine, 100 mg/l of L-threonine, 50 mg/l of L-isoleucine, 50 mg/l of L-valine, 60 mg/l of L-selenomethionine, incubation was continued for another 2.5 h. All amino acid vitamin solutions were filtered through a 0.22-µm filter (Sartorius). Protein expression was induced with IPTG at a final concentration of 1.0 mM. After incubation for 9 h at 15 °C with agitation at 800 rpm, cells were harvested by centrifugation. All of the subsequent steps were performed at 4 °C. The cells were resuspended in the described previously disruption buffer, and disrupted with French Press. SeMet-substituted PsoE was purified using essentially the same procedure as described above. The production of SeMet-substituted PsoE was confirmed with MALDI TOF MS.

1.5 *In vitro* analysis of the activity of PsoE and PsoF against 5.

The assay mixture (200 µl) containing 20 µM of purified PsoE or purified PsoE (20 µM) and PsoF (20 µM), 250 µM of **5**, 1 mM GSH, 1 mM FAD, 1 mM NADPH and 100 mM Tris-HCl (pH 7.4) was incubated at 30 °C for 30 min. Heat-inactivated samples of PsoE and PsoF were used in the indicated reaction as a negative control. After the 30-min incubation, the reaction mixture was quenched by addition of 250 µl of ethyl acetate including 3.3 µg/ml of *N*-Boc-L-tryptophan methyl ester as an internal standard (IS). The organic layer was separated by centrifugation, and the isolated organic fraction was dried *in vacuo*. For analyzing the production of **8**, the reaction mixture was quenched by addition of 250 µl of methanol. The mixture was centrifuged, and the supernatant was isolated. The dried material was dissolved in 100 µl of *N,N*-dimethylformamide (DMF) and subjected to LC–MS analysis performed with a Thermo SCIENTIFIC Exactive liquid chromatography mass spectrometer using both positive and negative electrospray ionization. LC was performed using an ACQUITY UPLC 1.8 µm, 2.1 × 50 mm C18 reversed-phase column (Waters) and separated on a linear gradient

of 10–50% (v/v) CH₃CN in H₂O supplemented with 0.05% (v/v) formic acid at a flow rate of 500 µl/min. Peak heights of different samples were standardized by scaling the peak height of *N*-Boc-L-tryptophan methyl ester used as an internal standard in all samples.

1.6 Additional *in vitro* analyses of the activities of PsoE and PsoF.

A solution with a total volume of 250 µl comprised of 10 µM each of nickel affinity-purified PsoE and PsoF (see **Figure S1B** and Tsunematsu *et al.*⁵, for production and purification of the recombinant PsoF), 50 µM of **5**, 0.1 M Tris-HCl (pH 7.4), 0.1 M NaCl and variable concentrations of GSH, FAD and NADPH was incubated at 30 °C for 30 min. After the incubation, the reaction mixture was quenched by addition of 250 µl of ethyl acetate including 3.3 µg/ml of *N*-Boc-L-tryptophan methyl ester as an internal standard. The organic layer was concentrated *in vacuo*. The dried material was dissolved in 100 µl of *N,N*-dimethylformamide (DMF) and subjected to liquid chromatography–mass spectrometry (LC–MS) analysis performed with a Thermo SCIENTIFIC Exactive liquid chromatography mass spectrometer using both positive and negative electrospray ionization. LC was performed using an ACQUITY UPLC 1.8 µm, 2.1 × 50 mm C18 reversed-phase column (Waters) and separated on a linear gradient of 10–50% (v/v) CH₃CN in H₂O supplemented with 0.05% (v/v) formic acid at a flow rate of 500 µl/min. The results of the analysis are given in **Figure S2**.

To follow the formation of GSH-conjugated intermediates, *in vitro* reactions were analyzed as described below. The assay mixture (200 µl) containing purified PsoE (20 µM) and PsoF (20 µM), 500 µM of **5**, a concentration of GSH varying from 10 µM to 1000 µM, 1 mM NADPH and H₂O was incubated at 30 °C for 1 h. Heat-inactivated samples of PsoE and PsoF were used in the indicated reaction as a negative control. After the 1-h incubation, the reaction mixture was quenched by addition of 250 µl of methanol. The mixture was centrifuged, and the supernatant was subjected to LC–MS analysis performed with a Thermo SCIENTIFIC Exactive liquid chromatography mass spectrometer using both positive and negative electrospray ionization. LC was performed using an ACQUITY UPLC 1.8 µm, 2.1 × 50 mm C18 reversed-phase column (Waters) and separated on a linear gradient of 10–50% (v/v) CH₃CN in H₂O supplemented with 0.05% (v/v) formic acid at a flow rate of 500 µl/min. The results of the analysis are given in **Figure S3**.

1.7 Protein crystallization and data collection.

A broad screening of crystallization conditions was performed for PsoE in the presence of GSH and **5** using a hanging drop method. Crystallization conditions that yielded microcrystals were reproduced and optimized in terms of pH, precipitant concentration and drop volume. The best crystal of the PsoE–GSH–**5** complex, i.e., the holo form of PsoE, were obtained by mixing 1.0 μ l of the protein (25 mg/ml) including 4 mM GSH and 2 mM substrate **5** with 1.0 μ l of a mother liquor of 30% PEGmme 5000, 150 mM $(\text{NH}_4)_2\text{SO}_4$ and 100 mM MES at pH 6.5. Crystals appeared after a few days at 20 °C and grew as needles. The crystal quality was further optimized using the Additive Screen kit (Hampton Research Corp.). The best quality crystal was obtained with an addition of 10 mM $[\text{Co}(\text{NH}_3)_6]\text{Cl}_3$ to the mother liquor. Prior to data collection, crystals were transferred to a cryoprotectant solution (15% ethylene glycol in the mother liquor) and immediately cryo-cooled in liquid nitrogen. Crystals of holo PsoE belong to the space group $P6_522$ and have one molecule per asymmetric unit. X-ray diffraction data were collected at Photon Factory and SPring-8 beamlines, and processed with the programs XDS⁶.

1.8 Structure refinement and model completion.

Phase was determined by the single-wavelength anomalous dispersion (SAD) method using the PHENIX AutoSol wizard⁷. The structure model was built with the program COOT⁸ and refined with phenix.refine⁹. Using the SAD-derived structure as a search model, native structures, both with and without cobalt ion, were determined by molecular replacement using the program Phaser¹⁰. The models were built with COOT⁸ and refined with phenix.refine⁹. Data collection and refinement statistics are shown in **Tables S2** and **S3**.

Table S1. Oligonucleotide primer sequences. DNA primers were designed on the basis of sequence data obtained from plasmid vector pET21c(+) and the *Aspergillus fumigatus* Af293 genome sequencing database.

| Primer name | Sequence |
|-------------|---|
| pKW20271-F1 | 5'- AGAAGGAGATATACAATGGTTTTTGGAACCTTGACACATTCCT -3' |
| pKW20271-R1 | 5'- GTGGTGGTGGTGGTGGTGGTGCCAGCCTGCGTAGCCTCAATAGCAACAG -3' |

2. Supporting Results

2.1. *E. coli* production of PsoE.

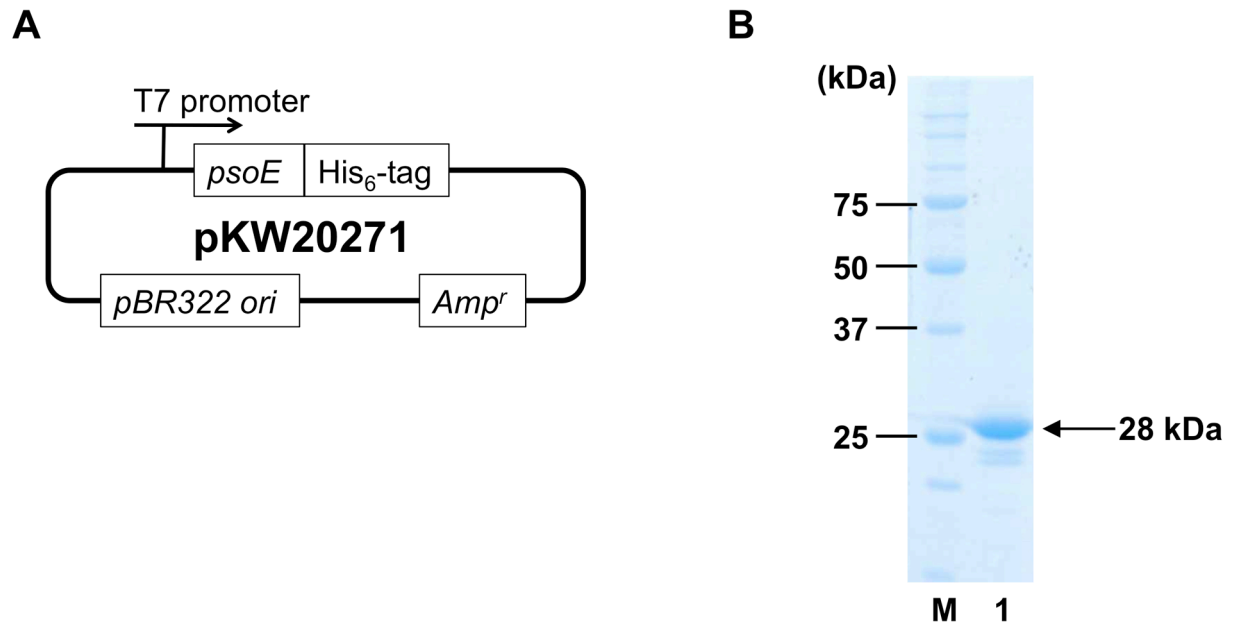


Figure S1. Production and purification of PsoE. (A) Map of plasmid pKW20271 for the production of PsoE in *E. coli*. (B) SDS-PAGE analysis of the purified PsoE stained with CBB. Lane M: molecular weight marker; lane 1: PsoE (28 kDa).

2.2. Additional *in vitro* analyses of the activities of PsoE and PsoF.

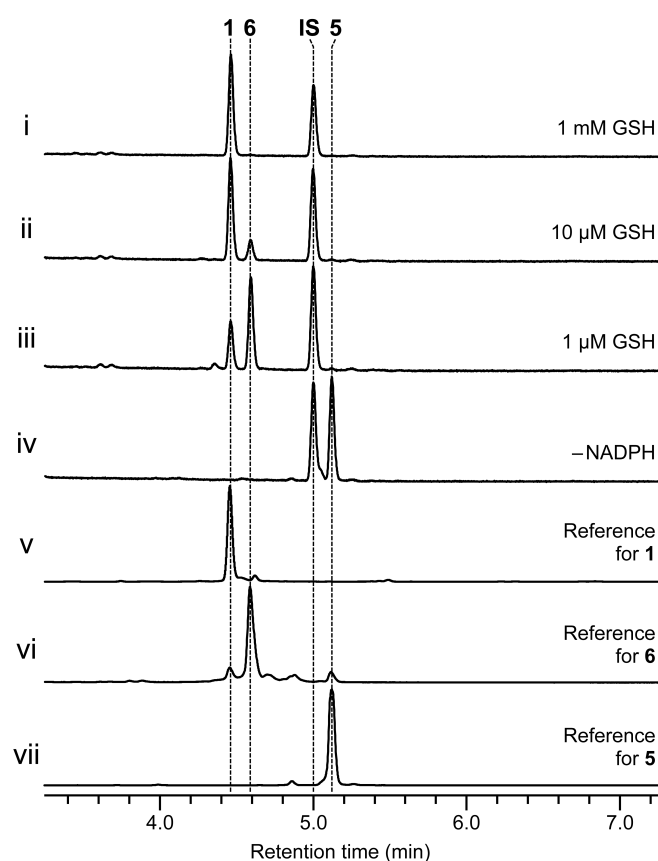


Figure S2. *In vitro* analysis of the activity of PsoE and PsoF against **5** (50 μM) for the formation of **1** and **6**. The HPLC traces were monitored at 280 nm. *N*-Boc-L-tryptophan methyl ester was used as an internal standard (IS) throughout the study. (i) Reaction with 1 mM GSH, 1 mM FAD and 1 mM NADPH. (ii) Reaction with 10 μM GSH, 0.1 mM FAD and 0.1 mM NADPH. (iii) Reaction with 1 μM GSH, 0.1 mM FAD and 0.1 mM NADPH. (iv) Reaction with 10 μM GSH and 0.1 mM FAD (i.e., no NADPH). The authentic reference of (v) **1**, (vi) **6** and (vii) **5** are also shown.

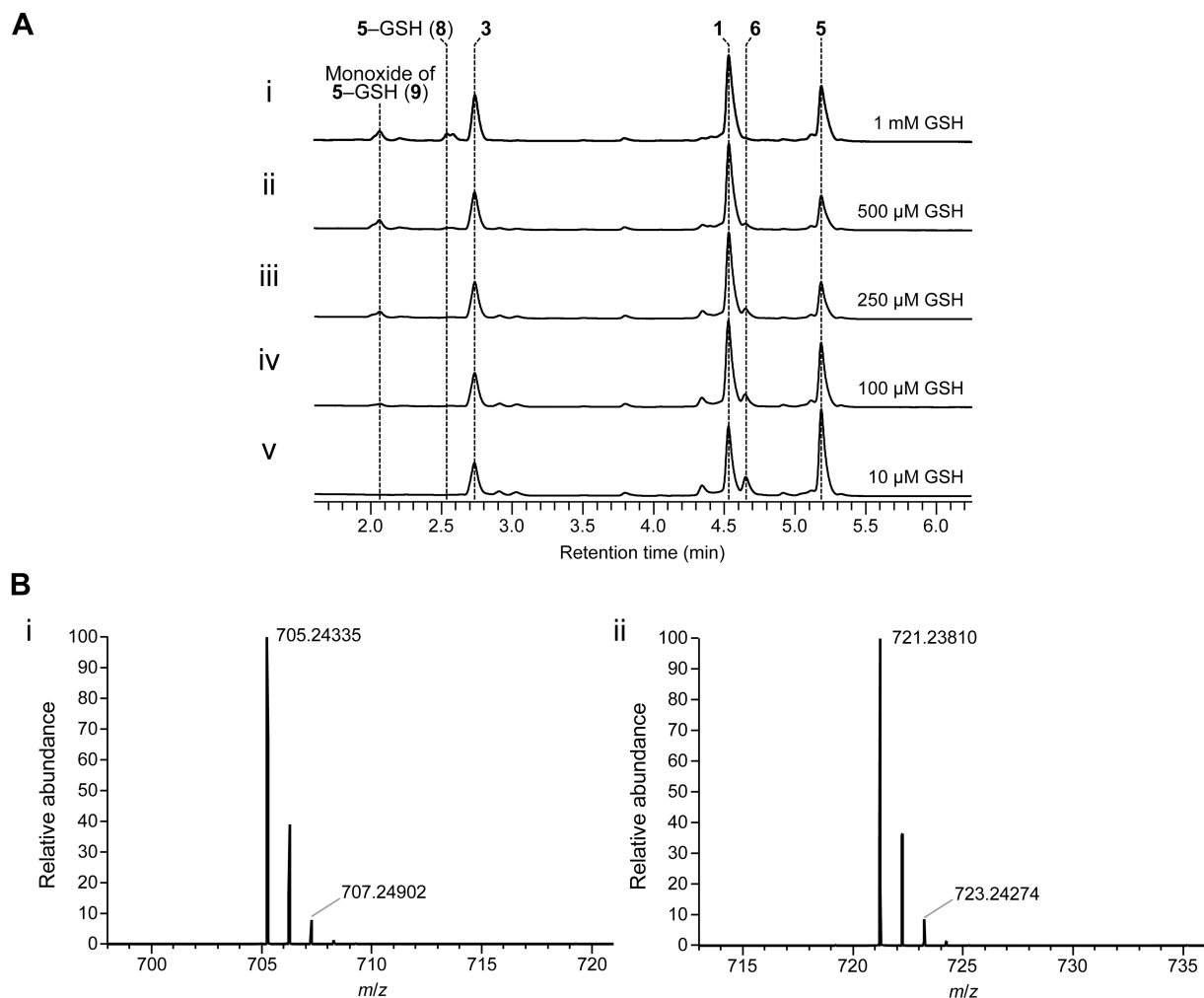


Figure S3. Analysis of the PsoE–PsoF *in vitro* assays against **5** (500 μ M) for the formation of GSH-conjugated intermediates. (A) HPLC traces (monitored at 280 nm) for reactions with (i) 1 mM GSH, (ii) 500 μ M GSH, (iii) 250 μ M GSH, (iv) 100 μ M GSH and (v) 10 μ M GSH. (B) Mass spectra corresponding to the m/z for (i) a **5**–GSH conjugate **8** [HRESIMS: m/z 705.2434 ($M+H$)⁺, calcd. for $C_{32}H_{41}N_4O_{12}S^+$, 705.2436, $\Delta = 0.2$ mmu] and (ii) a monoxide of the **5**–GSH conjugate, presumed sulfoxide intermediate **9** [HRESIMS: m/z 721.2381 ($M+H$)⁺, calcd. for $C_{32}H_{41}N_4O_{13}S^+$, 721.2385, $\Delta = 0.4$ mmu] extracted from the LC traces. Note, however, that a GSH conjugate of synerazol **1** also has the same m/z , and we cannot determine with certainty if the observed peak is comprised strictly of the **5**–GSH conjugate monoxide.

2.3. Glutathione-binding domain of amino acid sequence alignment.

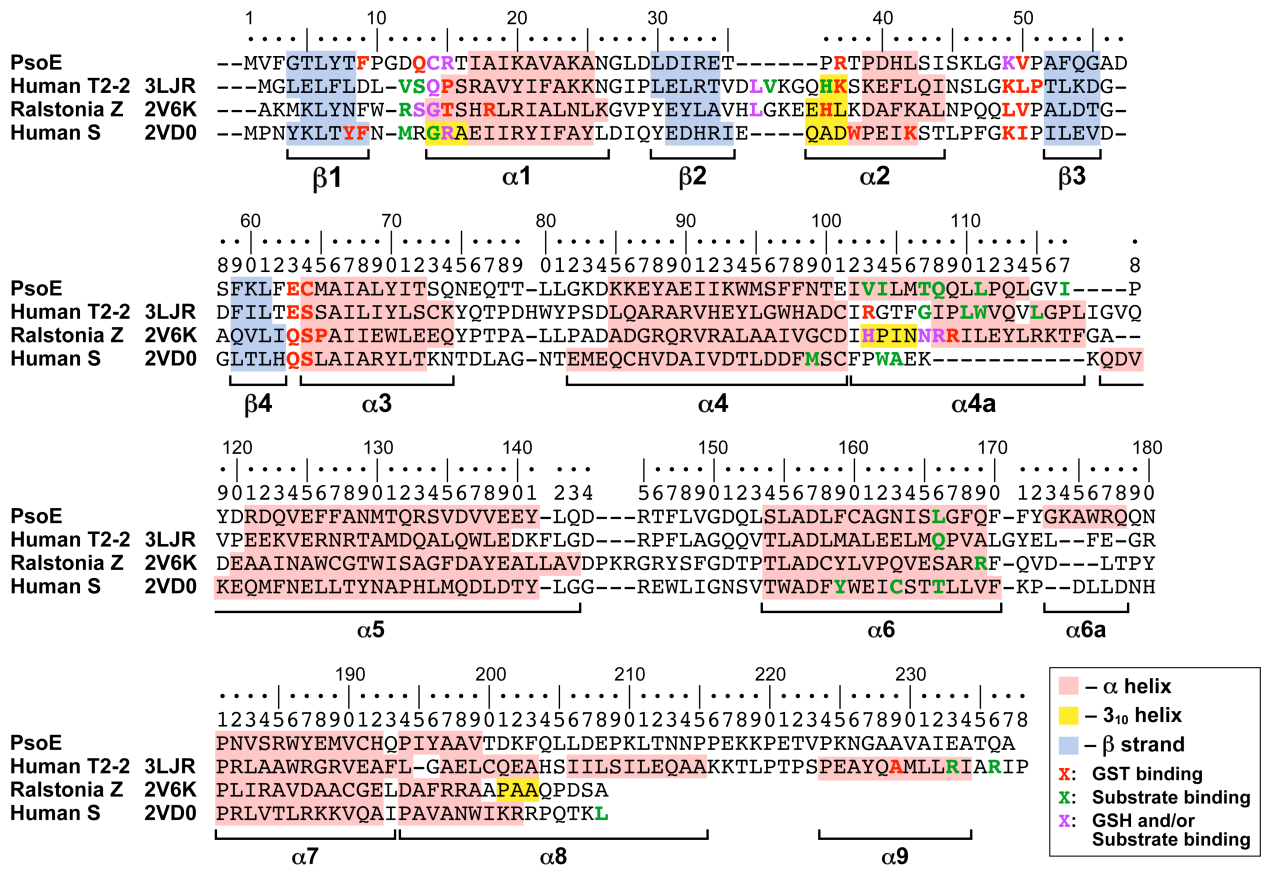


Figure S4. Structure-based amino acid sequence alignment of PsoE (NCBI GenPept accession number XP_747147), the theta class human GST T2-2B (NCBI GenPept accession number NP_001074312; PDB accession code 3LJR¹¹), the zeta class *Ralstonia* sp. strain U2 maleylpyruvate isomerase (NCBI GenPept accession number YP_009076550; PDB accession code 2V6K¹²) and the sigma class human hematopoietic prostaglandin D synthase (NCBI GenPept accession number NP_055300; PDB accession code 2VD0¹³). Residues involved in binding GSH, substrate and both are in bold and colored in red, green and magenta, respectively. Secondary structure elements α -helices, 3_{10} helices and β -strands are highlighted in pink, yellow and blue, respectively. Numbering is for the PsoE sequence.

2.4. Comparison of the ligand-binding mode in different GSTs.

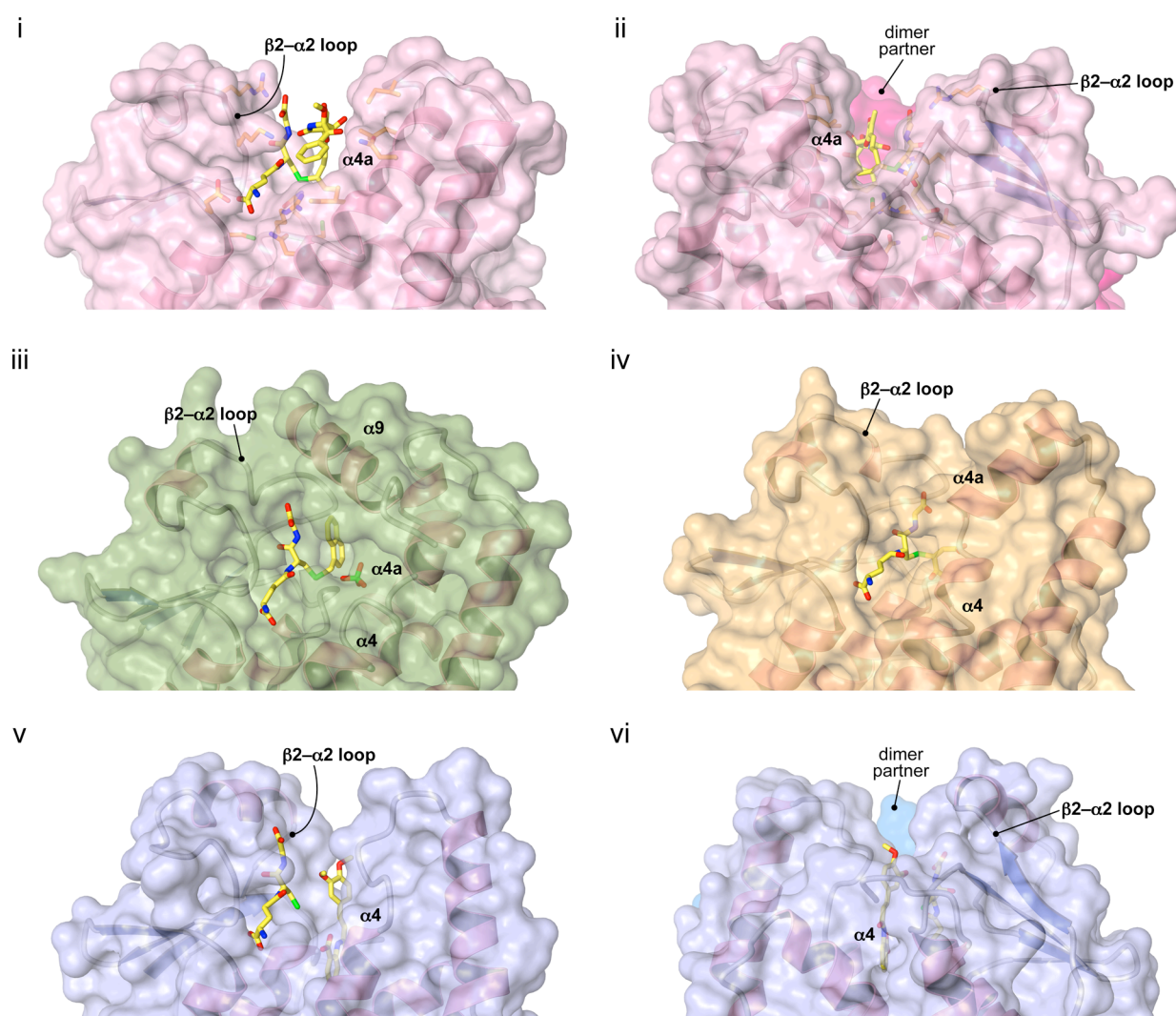


Figure S5. Comparison of the ligand-binding mode in different GSTs. Surface representation of PsoE and other GSTs is shown with their corresponding bound ligand drawn as a stick model. The ribbon diagram of the protein is shown through the semi-transparent surface. **(i)** PsoE monomer with bound **8a** viewed from the dimer interface; **(ii)** dimer of the PsoE–**8a** complex viewed roughly 180° rotated from the view in **(i)**; **(iii)** Theta GST, human T2-2 (PDB ID: 3LJR)¹¹ monomer with bound ligands 1-menaphthyl GSH and sulfate; **(iv)** Zeta GST, bacterial maleyl pyruvate isomerase (PDB ID: 2V6K)¹² monomer with bound ligand dicarboxyethyl glutathione; **(v)** Sigma GST, human prostaglandin D synthase (PDB ID: 2VD0)¹³ monomer with bound GST and an inhibitor tranilast viewed from the dimer interface; **(vi)** dimer of the Sigma GST–ligands complex viewed roughly 180° rotated from the view in **(v)**.

2.5. Effect of cobalt ion on packing of the ligand by PsoE.

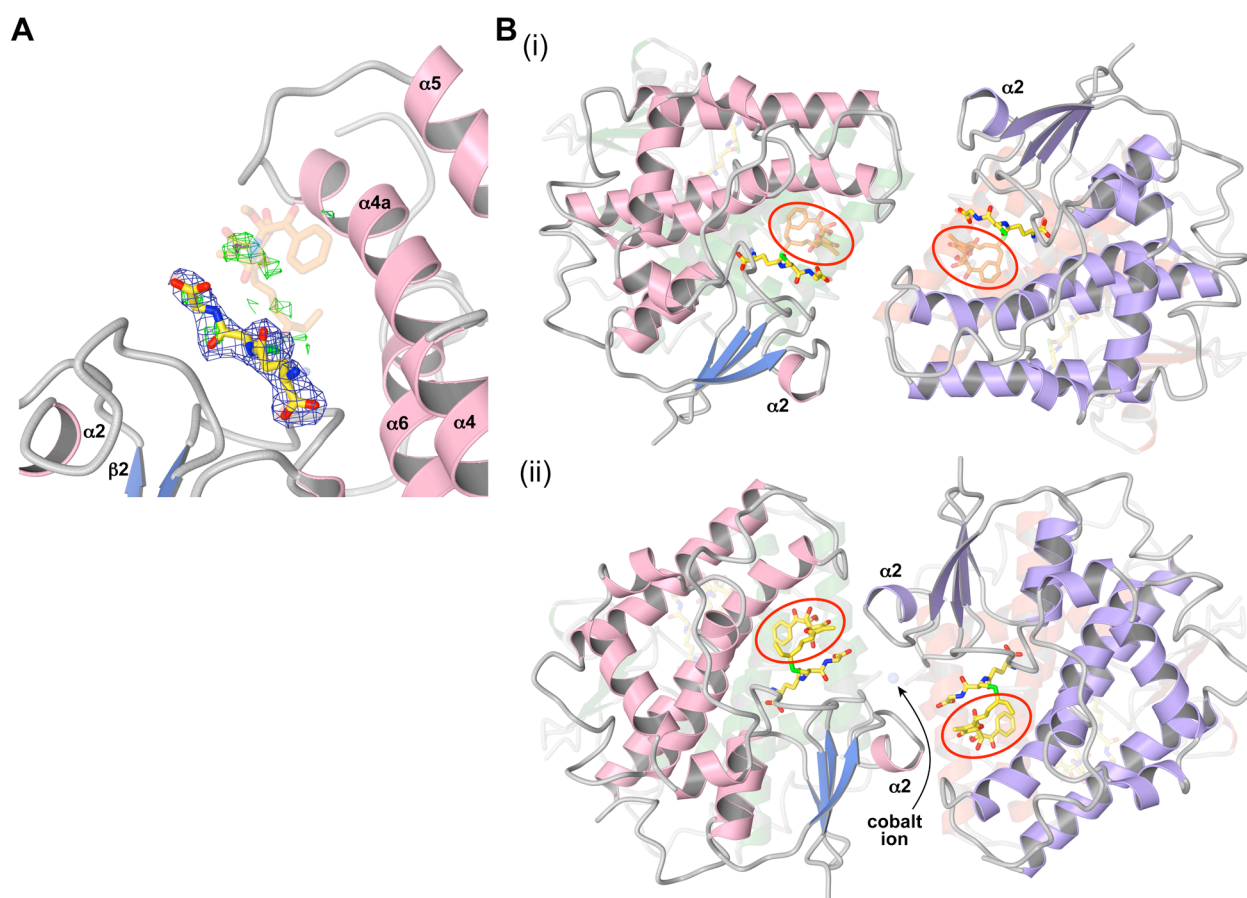


Figure S6. (A) The structure of PsoE-5-GSH complex determined with the crystal grown in the absence of cobalt ion. The GSH moiety is modeled, but the electron density for the 5 moiety is poor. The intact ligand 5-GSH (**8**) from the structure determined with the crystal grown in the presence of cobalt ion is superimposed (semitransparent). $2F_o - F_c$ map is shown in blue and contoured at 1.2σ . $F_o - F_c$ map is shown in green and contoured at 3.0σ . (B) Comparison of the packing of symmetry-related PsoE homodimers in the crystal grown in (i) the absence and (ii) the presence of cobalt ion. The dimer partner of the main monomer (left front) is colored in green (left back, faded). The symmetry-related monomer and its dimer partner are colored in purple (right front) and orange (right back, faded), respectively. In the cobalt-containing crystal, the $\alpha 2$ -containing loop is positioned near the active site of the symmetry-related molecule, restricting the movement of the bound 5 moiety (circled in red). On the other hand, symmetry-related molecules in the cobalt-free crystal are packed less tightly near the bound ligands, leaving a sufficient wiggle room for the bound 5 moiety.

Table S2. Data collection and structural refinement statistics on the PsoE–GSH–5 complex crystallized with cobalt ion. Values in parentheses are for the last resolution shell.

| Data Statistics | |
|---|--|
| | Native |
| Wavelength (Å) | 1.00000 |
| Space group | <i>P</i> 6 ₅ 22 |
| Unit cell dimensions | |
| a, b, c (Å) | 123.3, 123.3, 75.6 |
| α , β , γ (°) | 90.0, 90.0, 120.0 |
| Resolution (Å) | 50.0–2.54 (2.69–2.54) |
| Observed reflections | 245,397 (39,353) |
| Unique reflections | 21,209 (3,418) |
| R_{merge}^a | 10.0 (84.8) |
| Completeness (%) | 99.8 (99.9) |
| $I/\sigma(I)$ | 21.38 (3.39) |
| Redundancy | 11.57 |
| Molecules/asymmetric unit | 1 |
| Data collection facility | NW12A Photon Factory beamline, Tsukuba, JAPAN |
| Refinement Statistics | |
| Resolution (Å) | 43.62–2.54 (2.631–2.54) |
| Refined reflections | 21,156 |
| Free reflections | 2,100 |
| $R_{\text{work}}^b/R_{\text{free}}$ (%) | 19.12 / 24.67 |
| Ramachandran Prot | |
| Favored (%) | 96.71 |
| Allowed (%) | 3.29 |
| Outliers (%) | 0.00 |
| Number of atoms | |
| Protein | 1,730 |
| Ligands | 50 |
| Water | 12 |
| <i>B</i> -factors (Å ²) | |
| Protein | 61.70 |
| Ligands | 84.60 |
| Water | 53.10 |
| R.m.s. deviations | |
| Bond lengths (Å) | 0.015 |
| Bond angles (°) | 1.823 |
| Protein Data Bank code | 5F8B |

^a $R_{\text{sym}} = \sum |I_{\text{avg}} - I_i| / \sum I_i$, where I_i is the observed intensity and I_{avg} is the average intensity of observations of symmetry-related reflections.

^b $R_{\text{factor}} = \sum |F_p - F_{p(\text{calc.})}| / \sum F_p$, where F_p and $F_{p(\text{calc.})}$ are observed and calculated structure factors; R_{free} is calculated with 5% of the data.

Table S3. Data collection and structural refinement statistics on the PsoE–GSH–5 complex crystallized without cobalt ion. Values in parentheses are for the last resolution shell.

| Data Statistics | | |
|---|--|---|
| | Native | Se-peak |
| Wavelength (Å) | 1.10000 | 0.97867 |
| Space group | <i>P</i> 6 ₅ 22 | <i>P</i> 6 ₅ 22 |
| Unit cell dimensions | | |
| a, b, c (Å) | 145.413, 145.413, 51.266 | 145.2, 145.2, 50.4 |
| α, β, γ (°) | 90.0, 90.0, 120.0 | 90.0, 90.0, 120.0 |
| Resolution (Å) | 50.0–2.41 (2.56–2.41) | 20.0–3.16 (3.34–3.16) |
| Observed reflections | 248,692 (40,491) | 208,706 (28,694) |
| Unique reflections | 12,786 (1,991) | 10,085 (1,559) |
| R_{merge}^a | 8.5 (91.1) | 13.4 (78.2) |
| Completeness (%) | 99.8 (98.8) | 99.1 (97.5) |
| $I/\sigma(I)$ | 30.54 (3.89) | 24.72 (4.19) |
| Redundancy | 19.45 | 20.69 |
| Molecules/asymmetric unit | 1 | 1 |
| Data collection facility | BL-1A Photon Factory beamline, Tsukuba, JAPAN | BL-17A Photon Factory beamline, Tsukuba, JAPAN |
| Refinement Statistics | | |
| Resolution (Å) | 47.60–2.41 (2.46–2.41) | |
| Refined reflections | 23,385 | |
| Free reflections | 2,350 | |
| $R_{\text{work}}^b/R_{\text{free}}$ (%) | 18.47 / 24.56 | |
| Ramachandran Prot | | |
| Favored (%) | 95.77 | |
| Allowed (%) | 4.23 | |
| Outliers (%) | 0.00 | |
| Number of atoms | | |
| Protein | 1,730 | |
| Ligands | 20 | |
| Water | 24 | |
| <i>B</i> -factors (Å ²) | | |
| Protein | 57.30 | |
| Ligands | 73.30 | |
| Water | 46.90 | |
| R.m.s. deviations | | |
| Bond lengths (Å) | 0.015 | |
| Bond angles (°) | 1.448 | |
| Protein Data Bank code | 5FHI | |

^a $R_{\text{sym}} = \sum |I_{\text{avg}} - I_i| / \sum I_i$, where I_i is the observed intensity and I_{avg} is the average intensity of observations of symmetry-related reflections.

^b $R_{\text{factor}} = \sum |F_p - F_{p(\text{calc.})}| / \sum F_p$, where F_p and $F_{p(\text{calc.})}$ are observed and calculated structure factors; R_{free} is calculated with 5% of the data.

3. Supporting References

- (1) Johnson, M.; Zaretskaya, I.; Raytselis, Y.; Merezhuk, Y.; McGinnis, S.; Madden, T. L. *Nucleic Acids Res.* **2008**, *36*, W5.
- (2) Marchler-Bauer, A.; Lu, S.; Anderson, J. B.; Chitsaz, F.; Derbyshire, M. K.; DeWeese-Scott, C.; Fong, J. H.; Geer, L. Y.; Geer, R. C.; Gonzales, N. R.; Gwadz, M.; Hurwitz, D. I.; Jackson, J. D.; Ke, Z.; Lanczycki, C. J.; Lu, F.; Marchler, G. H.; Mullokandov, M.; Omelchenko, M. V.; Robertson, C. L.; Song, J. S.; Thanki, N.; Yamashita, R. A.; Zhang, D.; Zhang, N.; Zheng, C.; Bryant, S. H. *Nucleic Acids Res.* **2011**, *39*, D225.
- (3) Jaroszewski, L.; Li, Z.; Cai, X. H.; Weber, C.; Godzik, A. *Nucleic Acids Res.* **2011**, *39*, W38.
- (4) Yamamoto, T.; Tsunematsu, Y.; Noguchi, H.; Hotta, K.; Watanabe, K. *Org. Lett.* **2015**, *17*, 4992.
- (5) Tsunematsu, Y.; Fukutomi, M.; Saruwatari, T.; Noguchi, H.; Hotta, K.; Tang, Y.; Watanabe, K. *Angew. Chem. Int. Ed. Engl.* **2014**, *53*, 8475.
- (6) Kabsch, W. *Acta Crystallogr. D.* **2010**, *66*, 125.
- (7) Terwilliger, T. C.; Adams, P. D.; Read, R. J.; McCoy, A. J.; Moriarty, N. W.; Grosse-Kunstleve, R. W.; Afonine, P. V.; Zwart, P. H.; Hung, L. W. *Acta Crystallogr. D.* **2009**, *65*, 582.
- (8) Emsley, P.; Lohkamp, B.; Scott, W. G.; Cowtan, K. *Acta Crystallogr. D.* **2010**, *66*, 486.
- (9) Afonine, P. V.; Grosse-Kunstleve, R. W.; Echols, N.; Headd, J. J.; Moriarty, N. W.; Mustyakimov, M.; Terwilliger, T. C.; Urzhumtsev, A.; Zwart, P. H.; Adams, P. D. *Acta Crystallogr. D.* **2012**, *68*, 352.
- (10) McCoy, A. J.; Grosse-Kunstleve, R. W.; Adams, P. D.; Winn, M. D.; Storoni, L. C.; Read, R. J. *J. Appl. Crystallogr.* **2007**, *40*, 658.
- (11) Rossjohn, J.; McKinsty, W. J.; Oakley, A. J.; Verger, D.; Flanagan, J.; Chelvanayagam, G.; Tan, K. L.; Board, P. G.; Parker, M. W. *Structure* **1998**, *6*, 309.
- (12) Marsh, M.; Shoemark, D. K.; Jacob, A.; Robinson, C.; Cahill, B.; Zhou, N. Y.; Williams, P. A.; Hadfield, A. T. *J. Mol. Biol.* **2008**, *384*, 165.
- (13) Hohwy, M.; Spadola, L.; Lundquist, B.; Hawtin, P.; Dahmen, J.; Groth-Clausen, I.; Nilsson, E.; Persdotter, S.; von Wachenfeldt, K.; Folmer, R. H.; Edman, K. *J. Med. Chem.* **2008**, *51*, 2178.